JOURNAL OF INFORMATION SCIENCE AND ENGINEERING 22, 925-939 (2006)

A HVS-Directed Neural-Network-Based Approach for Salt-Pepper Impulse Noise Removal

SHIH-MAO LU[1], SHENG-FU LIANG AND CHIN-TENG LIN[1, 2]
[1]*Department of Electrical and Control Engineering*
[2]*Department of Computer Science*
Department of Biological Science and Technology
National Chiao Tung University
Hsinchu, 300 Taiwan

In this paper, a novel two-stage noise removal algorithm to deal with salt-pepper impulse noise is proposed. In the first stage, the decision-based recursive adaptive noise-exclusive median filter is applied to remove the noise cleanly and to keep the uncorrupted information as well as possible. In the second stage, the fuzzy decision rules inspired by human visual system (HVS) are proposed to classify image pixels into human perception sensitive class and non-sensitive class. A neural network is proposed to compensate the sensitive regions for image quality enhancement. According to the experimental results, the proposed method is superior to conventional methods in perceptual image quality as well as the clarity and the smoothness in edge regions of the resultant images.

Keywords: salt-pepper, impulse noise, noise removal, fuzzy decision system, human visual system, neural network

1. INTRODUCTION

Images are often corrupted by impulse noise due to noisy sensors or channel transmission errors. The objectives of noise removal are to suppress the impulse noise as well as to preserve the sharpness of edge and detail information. The standard median (SM) filter [1, 2] is a nonlinear filtering technique which has been extensively used and shown generally superior to linear filtering on suppressing impulse noise. However it tends to blur fine details and destroy edges while removing out the impulse noise. To achieve better performance, median filter has been modified in many ways, such as: center weighted median (CWM) filter [3], tri-state median (TSM) filter [4], multi-state median (MSM) filter [5], and recursive weighted median (RWM) filter [6], etc.

On the other hand, the family of median filters with adaptive-size by using one-dimensional and two-dimensional adaptive algorithms was developed in [7]. The recursive algorithm combined with median filter, which first replaces the gray level of each pixel with the output of the median filter before shifting the window to the next position, was proposed in [8] and [9]. In the decision-based scheme [10-12], median filtering is applied only to the pixels that are identified to be corrupted by noise. In addition, an edge-directed noise detection and suppression strategy has also been proposed in [13].

In this paper, a novel two-stage framework for salt-pepper impulse noise removal is

Received August 17, 2004; revised February 15 & June 17, 2005; accepted July 27, 2005.
Communicated by Liang-Gee Chen.

proposed. In the first stage, we employ the gray-level histogram statistics to detect the range of the salt-pepper impulse noise adaptively. Then the simple decision-based recursive adaptive median filter with 3×3 and 5×5 window sizes that only allows the clean pixel inside the window to participate in median processing is used to remove the impulse noise entirely and efficiently. In the second stage, an image quality enhancement system is proposed to compensate the destroyed pixels after the process of the first stage. It consists of a fuzzy decision system based on human visual system (HVS) for image analysis and a neural network for compensation.

This paper is organized as follows. Section 2 introduces system architecture of the proposed noise removal method. The decision-based recursive adaptive noise-exclusive median filter for noise removal is presented in section 3. The HVS-directed image analysis method and the neural network for image compensation are proposed in section 4. Section 5 presents the experimental results for demonstration and section 6 gives the conclusions of this paper.

2. SYSTEM ARCHITECTURE

In order to remove the noise pixels in an image without blurring the edge, we divide the process of noise removal into two stages. Fig. 1 shows the process flow of the first stage, called the decision-based recursive adaptive median filtering scheme. The noise range estimation and decision-based rules decide whether the pixel is possibly corrupted by the noise, and the median filter is applied only to the possibly noise-corrupted pixels. The window size of median filter is chosen depending on how heavily the neighboring pixels are corrupted by noise such that we can remove the noise entirely without heavily destroying the details of the image. The recursive algorithm replaces the value of median filter before the window shifts to next possible noise pixel and the noise-exclusive scheme allows only the clean pixels inside the window to participate in median processing such that we can remove the noise as clean as possible.

The schematic block diagram of the image quality enhancement system in the second stage is shown in Fig. 2. Based on the fuzzy decision, either the filtered value of the first stage or the result of adaptive neural-network compensation module is selected to compensate each noise corrupted pixel. When the adaptive neural-network compensation is actuated, the angle evaluation module will compute the dominant orientation of the original image located in the sliding block as the input data of the proposed neural network.

When an image has been processed in the first stage, the second-stage process starts. The image is firstly divided into the 4×4 sliding (overlapping) blocks. The weighted compensation is applied to the visual-sensitive region and can be presented as:

$$F(m, n) = \sum_{i=-1}^{2} \sum_{j=-1}^{2} O(m+i, n+j) W_{\theta}(i, j), \tag{1}$$

where $O(m, n)$ is the reference pixel that possibly corrupted by noise, $O(m + i, n + j)|_{i\neq 0, j\neq 0}$ are the neighborhoods of $O(m, n)$ and W_{θ} are the weights of training results.

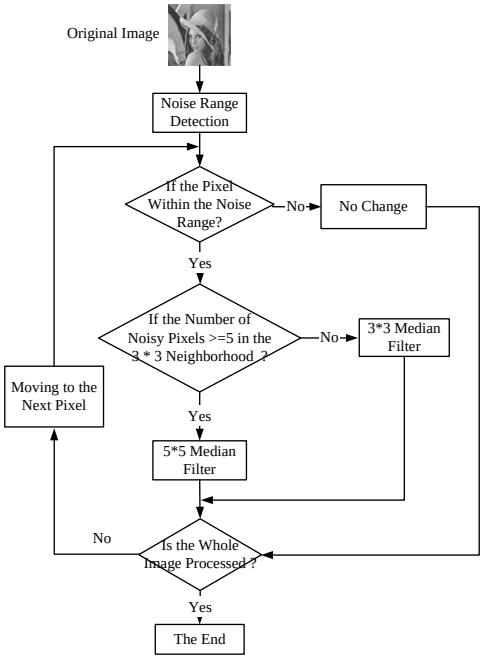

Fig. 1. The decision-based adaptive recursive median filtering scheme.

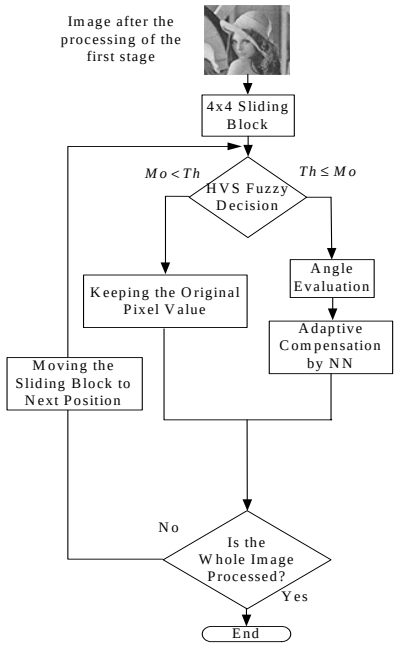

Fig. 2. Schematic block diagram of the proposed image quality enhancement system.

3. IMPULSE NOISE REMOVAL

In the first stage, the goal is to remove the impulse noises and to keep the detailed information of the processed image as much as possible so that we can compensate the noise corrupted pixels well by using their neighbors in the second stage. The techniques used in the first stage are introduced as follows.

3.1 Noise Range Estimation

The noise model used in this paper is the additive salt-pepper impulse noise that is a popular and practical case in image processing. Conventionally, it assumes 0 for negative impulse (pepper noise) and 255 for positive impulse (salt noise). In a more practical situation, the noise pixels are corrupted by the noise with pixel values equal to or near the maximum or minimum value in the allowable dynamic range and this noise model is also adopted in this paper. In addition, if the original image is corrupted by the additive salt-pepper impulse noise with probability p, the probabilities of positive noise and negative noise are identical, i.e., $p/2$.

According to histogram analysis, there is a gap between the gray values of noise pixels and gray values of the normal pixels. Therefore, we apply the gap detection to the histogram to estimate the noise ranges near the maximal and minimal gray levels adaptively. Defining *ThL* as the gap threshold for pepper noise (negative impulse) and *ThH* as the gap threshold for salt (positive impulse) noise, they can be calculated by

$$ThL = \{h \mid \max(His(h) - His(h+1)), \text{ from } h = 0 \text{ to } 128\}, \quad (2)$$

$$ThH = \{h \mid \max(His(h+1) - His(h)), \text{ from } h = 255 \text{ to } 128\}, \quad (3)$$

where $His(h)$ is the histogram of the noisy image at gray level h. The initial values of ThH and ThL are set as 256 and – 1 to deal with the case that images are corrupted with either salt or pepper noise. If the gray level of a pixel is within the noise range, which is smaller than ThL or greater than ThH, we classify it as a suspected noise pixel and execute noise removal process as shown in Fig. 1.

3.2 Decision Rules

As a matter of fact, most of the pixels in the noisy image are uncorrupted and pixel values should not be changed. In noise detection step, each pixel is classified into the possible noise pixel or the uncorrupted pixel. In our strategy, the pixels within the determined noise range are regarded as possible noise-corrupted pixels and they will be processed by the adaptive noise-exclusive median filter. The uncorrupted pixels are retained without any modification to avoid blurring caused by unnecessary processing. In such decision rule, noise pixels will be completely detected but the original pixels in these intervals will also be false identified as noise pixels. Although some pixels are falsely detected, most of them are in the smooth regions and their gray levels are very close to the nearby pixels, so the result of median filtering will not destroy the image quality too much. Even if the falsely detected pixels are in the edge area, our second stage, image quality enhancement, will compensate the jaggy edges well.

3.3 The Adaptive Noise-Exclusive Median Filtering

When images are highly corrupted with noise, several noise pixels may connect into noise blotches so that they cannot be removed by the median filter with small window size (such as 3×3). On the other hand, when the median filter with large window size (such as 5×5) is employed to image processing, it often causes edge blurring.

In this paper, an adaptive median filter is proposed to achieve superior performance of noise suppression as well as preserving more detailed information. We first analyze the neighboring 3×3 region of the possible noise pixels. If there are more than four other possible noise pixels in this block, it is identified as the highly corrupted region and the 5×5 median filter is applied for processing. Otherwise, the 3×3 median filter is applied to this pixel. In addition, the noise-exclusive scheme is also used in this paper to remove the noise cleanly. It allows only the clean pixels inside the window to participate in the median processing.

3.4 Recursive Method

The recursive algorithm replaces the value of the noise pixel with the processing output of the adaptive median filter before the window shifts to the next noise pixel [9]. It can efficiently reduce the number of noise pixels and remove the noise more cleanly. The drawback of the recursive algorithm is that it will blur the edges and detailed infor-

mation. Therefore, the second stage of the proposed method, image quality enhancement, is necessary for compensation.

4. IMAGE QUALITY ENHANCEMENT

It is well known that conventional median filtering techniques often suffer from blurring details and cause artifacts around edges. In order to compensate the edge sharpness, image quality enhancement is applied to the processed pixels. For image analysis, we make use of the properties of human visual system (HVS) to obtain the features of images such that we could realize which region is worth further quality enhancement, since human eyes are usually more sensitive to this region. An adaptive neural network is also proposed to compensate the pixels in the sensitive region for image quality enhancement.

4.1 HVS-Directed Image Analysis

Many researches have been made on discovering the characteristics of HVS for years. It was found that the perception of HVS is more sensitive to luminance contrast rather than the uniform brightness [14]. In addition to the magnitude difference between object and the background, different structures of images also cause different visual perceptions for HVS. Many features have been proposed based on the block DCT in frequency domain. In this paper, a novel fuzzy decision system inspired by HVS is proposed to classify the image into human perception sensitive and non-sensitive regions in spatial domain. There are three input variables, visibility degree (VD), structural degree (SD), complexity degree (CD), and one output variable (Mo) in the proposed fuzzy decision system.

The first input variable of the fuzzy decision system, VD, is related to the ability of human eyes to tell the magnitude difference between an object and its background depending on the background luminance. Fig. 3 shows the actual visibility thresholds called just-noticeable-distortion (JND) corresponding to different background luminance and it was verified by a subjective experiment [14]. We can find that the visibility threshold is lower when the background luminance is within the interval from 70 to 150, and the visibility threshold will rise if the background luminance becomes darker or brighter away from this interval.

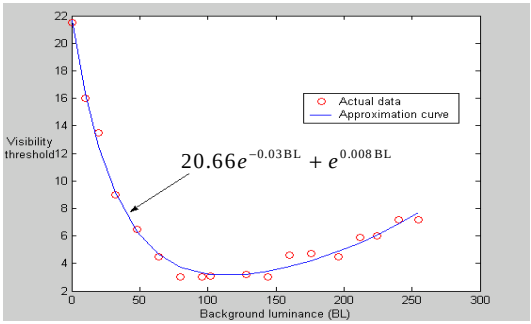

Fig. 3. Visibility thresholds corresponding to different background luminance.

In order to obtain the variable VD, two index parameters called background luminance (BL) and difference (D) are defined at first. BL is the average luminance of the sliding block proposed to approximate the actual background luminance and can be calculated by

$$BL = \frac{1}{23}\sum_{i=-1}^{2}\sum_{j=-1}^{2} O(i, j)\times B(i, j), \tag{4}$$

where

$$B(i, j) = \begin{bmatrix} 2 & 2 & 2 & 1 \\ 2 & 0 & 2 & 1 \\ 2 & 2 & 2 & 1 \\ 1 & 1 & 1 & 1 \end{bmatrix}, \tag{5}$$

and the denominator 23 in Eq. (4) is the weighted sum of all elements in Eq. (5) for normalization. Feature D is the difference between the maximum pixel value and the minimum pixel value in the sliding block and can be calculated by

$$\mathrm{D} = \max(O(i, j)) - \min(O(i, j)). \tag{6}$$

A nonlinear function V(BL) is also designed to approximate the relation between the visibility threshold and background luminance [14] (as shown in Fig. 3), and can be represented as:

$$\mathrm{V(BL)} = 20.66e^{-0.03\mathrm{BL}} + e^{0.008\mathrm{BL}}. \tag{7}$$

VD is defined as the difference between D and V(BL) and can be represented as

$$\mathrm{VD} = \mathrm{D} - \mathrm{V(BL)}. \tag{8}$$

If VD > 0, it means the magnitude difference between the object and its background exceeds the visibility threshold and the object is sensible. Otherwise, this object is not sensible.

The other two input variables, SD and CD, are used to indicate whether the pixels in the sliding block own edge structure.

SD shows if the sliding block is a high contrast region and the pixels in the block can be obviously separated into two clusters. It is calculated by

$$\mathrm{SD} = \frac{|\max(O(i, j)) - \mathrm{mean}(O(i, j)) - [\mathrm{mean}(O(i, j)) - \min(O(i, j))]|}{\max(O(i, j)) - \mathrm{mean}(O(i, j))}, \tag{9}$$

where

$$\mathrm{mean}(O(i, j)) = \frac{1}{16}\sum_{i=-1}^{2}\sum_{j=-1}^{2} O(i, j). \tag{10}$$

If SD is a large value, it means the numbers of pixels in these two clusters are not even. Thus the block may contain noise. On the other hand, if SD is small, the numbers of pixels in these two clusters are even and the block may contain edge or texture structure.

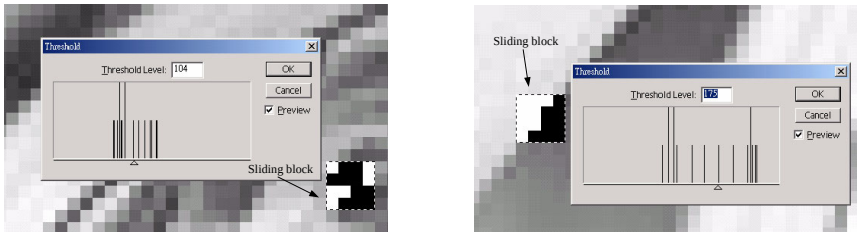

(a) (b)

Fig. 4. Portions of (a) the sliding block containing texture structure, (b) the sliding block containing edge structure.

Figs. 4 (a) and (b) show a texture structure and a delineated edge structure in a sliding block, respectively. In these two plots, the numbers of pixels in these two clusters are the same. Therefore, the SD values corresponding to these two structures are close. Since the proposed neural network is used to compensate the sensitive regions such as Fig. 4 (b), CD input variable based on differential process is employed to tell the delineated edge structure from texture structure. It is calculated by

$$\mathrm{CD} = \sum_{i=-1}^{2} \sum_{j=-1}^{2} |\, 4O'(i,\, j) - [O'(i+1,\, j) + O'(i-1,\, j) + O'(i,\, j+1) + O'(i,\, j-1)]\,|, \qquad (11)$$

where $O'(i, j)$ is the binarized version of $O(i, j)$. Assuming mean(O) is the mean gray level of the sliding block, $O'(i, j)$ is defined as:

$$O'(i,\, j) = \begin{cases} 1, & \text{if } O(i,\, j) \geq \mathrm{mean}(O), \\ 0, & \text{otherwise.} \end{cases} \qquad (12)$$

In Eq. (11), each pixel in the 4×4 sliding block takes the 4-directional local gradient operation and CD is the summation of the 16 local gradient values. If CD is a large value, it means the block may contain texture structure. On the contrary, if CD is a small value, the block may contain delineated edge structure.

In the proposed HVS-based Fuzzy decision system, the input variable VD has two fuzzy sets, N (negative) and P (positive). The input variable SD has three fuzzy sets S (small), M (medium), and B (Big). The input variable CD has three fuzzy sets, S (small), M (medium), and B (Big). The membership functions, corresponding to VD, SD, and CD, are chosen by experiments as shown in Figs. 5 (a-c), respectively.

In order to determine the fuzzy membership functions, seven nature images were used to generate the model. The images were separated into smooth, texture and edge regions by the admission of the majority (seven of ten subjects). Then the ranges of VD,

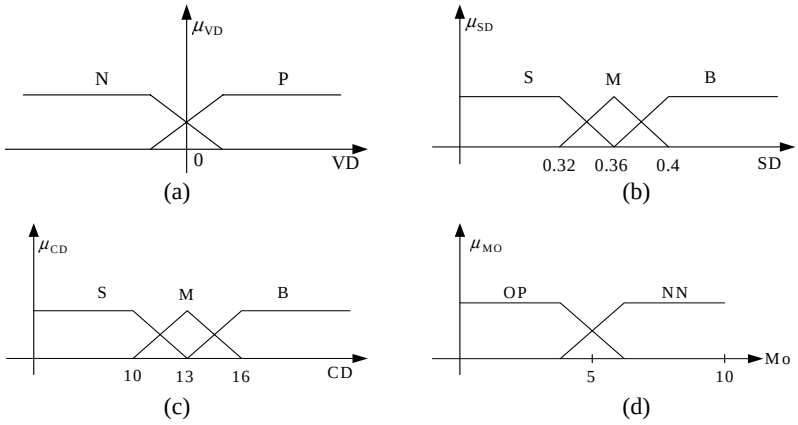

Fig. 5. (a)-(d) Membership functions of fuzzy sets on input variables VD, SD, CD, and output variable Mo, respectively.

CD and SD proposed in Eqs. (8), (9) and (11) corresponding to these regions were evaluated. Finally, the membership functions of VD, CD and SD could be designed according to the distribution ranges of the parameters in these regions, respectively. Mo is the output variable and the membership functions corresponding to Mo are shown in Fig. 5 (d). It has two fuzzy sets, NN (neural network) and OP (original pixel).

Seven fuzzy decision rules are used in the proposed fuzzy system and represented as follows:

1. If VD is N then Mo is OP
2. If SD is B then Mo is OP
3. If CD is B then Mo is OP
4. If VD is P and SD is S and CD is S then Mo is NN
5. If VD is P and SD is S and CD is M then Mo is NN
6. If VD is P and SD is M and CD is S then Mo is NN
7. If VD is P and SD is M and CD is M then Mo is OP.

The numerical value of Mo after COA defuzzification is compared with a threshold value, Th, where Th is preferably set as 5 by experiments. When Mo ≥ Th, the adaptive neural-network (NN) compensation module with angle evaluation would be chosen. Otherwise, the original pixel (OP) value would be used.

4.2 Angle Evaluation

As Mo ≥ Th, the fuzzy system identifies the reference pixel as sensible delineated edge and the trained adaptive neural-network model is chosen for quality enhancement according to its corresponding edge angle. The angle evaluation shown in Fig. 6 is performed to determine the dominant orientation of the sliding block. It firstly computes the orientation angle of each neighborhood of the original image pixel. The orientation angle of $O(i, j)$ denoted as $A(i, j)$ is computed by the following equations:

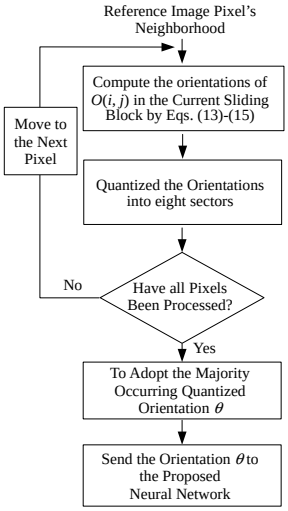

Fig. 6. Flow diagram of the angle evaluation.

$$Dx(i,j) = O(i-1,j-1) + 2O(i-1,j) + O(i-1,j+1) - (O(i+1,j-1) + 2O(i+1,j) + O(i+1,j+1)), \quad (13)$$

$$Dy(i,j) = O(i-1,j-1) + 2O(i,j-1) + O(i+1,j-1) - (O(i-1,j+1) + 2O(i,j+1) + O(i+1,j+1)), \quad (14)$$

$$A(i,j) = -\frac{180}{\pi}\left[\tan^{-1}\left(\frac{Dy(i,j)}{Dx(i,j)}\right)\right], \quad (15)$$

where $-1 \le i \le 2$ and $-1 \le j \le 2$.

The obtained angle of each pixel in the sliding window is quantized into eight quantization sectors such as $\theta = 22.5 \times k$ degrees, where $k = 0, 1, \ldots, 7$. We adopt the majority quantized angle in the sliding block regarded as the dominant orientation θ of the reference edge pixel. Finally, the corresponding weighting coefficient W_θ derived from the off-line training neural network is adopted for compensation.

4.3 Neural-Network-Based Image Compensation

The function of the proposed neural network is to obtain the weights W_θ defined in Eq. (1), where θ represents the quantized dominant orientation of the reference pixel. Thus, the proposed neural network is used to obtain 8 sets of weighting matrices through training. Each weighting matrix W_θ can be represented as

$$W_\theta(i,j) = \begin{bmatrix} w_{-1-1} & w_{-10} & w_{-11} & w_{-12} \\ w_{0-1} & w_{00} & w_{01} & w_{02} \\ w_{1-1} & w_{10} & w_{11} & w_{12} \\ w_{2-1} & w_{20} & w_{21} & w_{22} \end{bmatrix}. \quad (16)$$

In order to use supervised learning algorithms to train the proposed neural network, we have to obtain the desired input-output patterns such that the differences of network outputs and the corresponding desired outputs can be used to define the cost function as the goal to minimize. In this section, several clean image portions with dominant orientation are used as the training patterns. Assuming a clean image portion is denoted as I, the noise-corrupted version of I has been processed by the proposed noise removal method in the first stage and the filtered result is denoted as I'. Let $I'(i, j)$ be the reference pixel, where $O(m, n) = I'(i, j)$, and it is classified as an edge pixel with dominant orientation θ after angle evaluation.

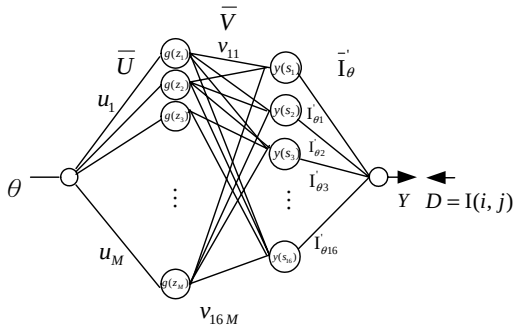

Fig. 7. The proposed feed-forward neural network for image quality enhancement.

A new neural network as shown in Fig. 7 is proposed for image compensation. It is a 4-layer network with two hidden layers. The input of the neural network is defined as θ, and the network output is the compensated pixel value of $I'(i, j)$. When the input-output patterns are given, the following task is to train a neural network to match the input-output relations. The second layer (1st hidden layer) consists of M nodes denoted as $g(z_i)$, where M is 200 in our experiments, and the bipolar sigmoid function is used as the activation function. The weighting vector between the first and the second layers is denoted as $\overline{U}$. The third layer (2nd hidden layer) includes 16 nodes and the bipolar sigmoid function is also used as the activation function. The weighting vector between the second and the third layers is denoted as $\overline{V}$. The output value of each node in the third layer is denoted as $y(s_l)$ and represents an element of the weighting matrix W_θ given in Eq. (16), where $y(s_l) = w_{ij}$, $l = 4i + j + 6$, $1 \le l \le 16$, $-1 \le i \le 2$, and $-1 \le j \le 2$. The fourth layer is the output layer with one output node and its output value represents the compensated pixel value of $I'(i, j)$. The vector between the third and the fourth layers is denoted as $\overline{I}'_\theta$. It represents the vector of the sixteen neighborhood pixels of the reference pixel $I'(i, j)$ with dominant orientation θ as follows:

$$\overline{I}'_\theta = \begin{bmatrix} I'_{\theta 1} \\ I'_{\theta 2} \\ I'_{\theta 3} \\ I'_{\theta 4} \\ I'_{\theta 5} \\ \vdots \\ I'_{\theta 16} \end{bmatrix} = \begin{bmatrix} I'(i-1, j-1) \\ I'(i, j-1) \\ I'(i+1, j-1) \\ I'(i+2, j-1) \\ I'(i-1, j) \\ \vdots \\ I'(i+2, j+2) \end{bmatrix}. \tag{17}$$

Then the estimated output of the system can be calculated by

$$Y = \sum_{l=1}^{16} y(s_l) \cdot \mathrm{I}'_{\theta\, l} \tag{18}$$

and the corresponding desired output D can be obtained by

$$D = I(i, j). \tag{19}$$

It should be noted that the weighting vectors need to be updated in the training stage are only $\overline{V}$ and $\overline{U}$. If a reference pixel $I'(i, j)$ is given, the neighborhood pixel vector $\overline{I}'_{\theta}$ of $I'(i, j)$ can be regarded as an extra input vector for compensation.

In the training stage, the updating rules of weights, $v_{ab} \in \overline{V}$, $ub \in \overline{U}$, can be derived by the back-propagation learning method as

$$v_{ab}(t + 1) = v_{ab}(t) + \eta\,(D - Y)[I'_{\theta a}\,(1 + y(s_a))(1 - y(s_a))/2] \times g(Z_b), \tag{20}$$

$$u_b(t+1) = u_b(t) + \eta\left\{\sum_{i=1}^{16}\left[(D-Y)(I'_{\theta i})\frac{(1+y(s_i))(1-y(s_i))}{2}v_{ib}\right]\right\} \times[(1+g(Z_b))(1-g(Z_b))/2]\times IP, \tag{21}$$

where $\eta = 0.2$ is the learning constant which determines the learning rate and IP is the input of the network. Thirty nature images were used to train the proposed neural network for image compensation. The goal is to reduce the cost function (MSE) to 1% of the intensity range, i.e. $255 \cdot 0.01 \cong 2.5$. When the training process is finished, 8 different input values, θ, can be inputted to the trained network, and the corresponding weighting matrices W_θ can be obtained to build a look up table for image compensation to reduce the computational cost.

5. EXPERIMENTAL RESULTS

The performance of the proposed method has been examined on a variety of testing images corrupted with various noise densities and quantitatively measured by the peak signal-to-noise ratio (PSNR). In our experiments, the proposed algorithm is compared with five existing methods including median filter [1], recursive median filter [2], Center Weighted Median (CWM) Filter [3], Tri-State Median Filter [4], and Li's method [13].

The testing results of Lena with 40% impulse noise are shown in Fig. 8. According to Figs. 8 (c) and (d), we can find the recursive median filter removes the noise well but also blurs the edge, so the recursive algorithm cannot balance the noise removal and edge sharpness well. In Figs. 8 (e) and (f), the Tri-State Median can retain more edge sharpness than the CWM, but both of them cannot remove the noise very well in some highly noise-corrupted area. In Fig. 8 (g), Li's method might misjudge some noise pixels as the edge and then increase the size of some noises. It shows that the proposed method can effectively remove the noise and keep the edge sharpness well.

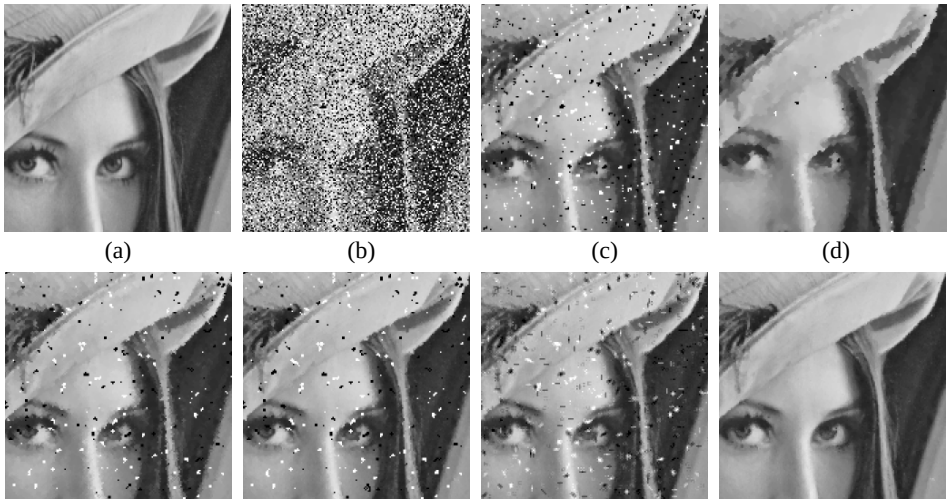

(a) (b) (c) (d)

(e) (f) (g) (h)

Fig. 8. (a) Original Lena image; (b) Lena with 40% of impulse noise; (c) The 3×3 standard median filter; (d) The 3×3 recursive standard median filter; (e) The recursive CWM filter with weight = 3; (f) The recursive Tri-state median filter with threshold = 25; (g) Li's method with threshold = 32; (h) Our proposed method.

Table 1. Quantitative comparisons of different noise removal methods applied to the images with various percentages of impulse noise.

Filters	Images Corrupted with 40 % Impulse Noise					
	Lena	Peppers	Sailboat	Baboon	Aerial	Boat
Median	19.13	18.70	18.28	17.31	17.79	18.67
R-Median	26.86	25.79	23.45	20.69	22.01	24.84
CWM 3 [3]	20.18	19.54	19.02	18.30	18.64	19.56
Tri-State [4]	20.26	19.55	19.13	18.43	18.74	19.65
Li [13]	22.02	21.47	20.73	19.12	19.94	21.22
After our 1st- stage processing	34.05	32.80	30.10	24.96	27.57	31.71
The complete processing of our method	35.66	33.69	30.55	25.20	28.05	32.78

(a) (b) (c) (d)

Fig. 9. (a) Original Lena image; (b) Lena with 40% of impulse noise; (c) Resultant image after the processing of the 1st stage (impulse noise removal); (d) Resultant image after the processing of 2nd stage (image quality enhancement).

Fig. 9 and Table 2 show the indispensability of the noise removal stage to remove the noise well and the image quality enhancement stage to compensate the blur and jaggy edge. Because we take the advantages of noise-exclusive scheme and the median filter with adaptive-size well, the proposed first-stage processing is so powerful in removing the impulse noise. The noise-exclusive scheme that allows only uncorrupted pixels inside the window to participate in median processing effectively improves the noise suppression ability. When images are highly corrupted by the noise, several pixels may connect into noise blotches. Therefore, more 5×5 median filter is employed to remove the noise pixels.

The hardware and software environment that we implement the algorithms for speed comparison are described as follows: all the algorithms are implemented in Matlab Language on a 1.8G Hz Pentium IV-based PC with 256 MB RAM. Table 3 shows the average computation time in second for various algorithms applied to different kinds of noise corrupted images. The time consuming of the proposed algorithm is quite reasonable compared with other methods.

Table 2. Compensation ability of our adaptive median filter in the 1st stage and the image quality enhancement system in the 2nd stage with respect to Lena.

Impulse Noise Ratio	5 %	10 %	20 %	40 %
Percentage of 5×5 Median filter used in the 1st stage	0%	0.05%	0.31%	3%
PSNR after the processing of the 1st stage	45.60	42.12	38.40	34.05
PSNR after the processing of the 2nd stage	46.26	43.08	39.74	35.66
Total pixels of Mo>Th	8595	16525	33428	65651
Total pixels corrupted by the noise	13218	26007	52813	104868

Table 3. Speed comparison for various algorithms (unit: sec).

Algorithm	Median	R-Median	CWM 3	TRI	Li's	The Proposed
Ave. Time (sec.)	52	54	53	100	700	120

6. CONCLUSIONS

In this paper, a novel two-stage noise removal algorithm for salt-pepper impulse noise removal is proposed. In the first stage, the adaptive decision-based recursive median filter is applied to remove the noise cleanly and to keep the uncorrupted information as well as possible. In the second stage, the fuzzy decision rules inspired by human visual system (HVS) are proposed to classify pixels of the image into human perception sensitive class and non-sensitive class. According to the experiment results, the proposed method is superior to the existing methods in both the quantitative and the visual qualitative performance. In addition, the proposed fuzzy decision rules combined with the neural network can balance the trade-off between speed and quality for different applications by just adjusting a threshold parameter.

REFERENCES

1. T. A. Nodes and N. C. Gallagher, "Median filters: Some modifications and their Properties," *IEEE Transactions on Acoustics, Speech, Signal Processing*, Vol. ASSP-30, 1982, pp. 739-746.
2. G. R. Arce and R. J. Crinon, "Median filters: analysis for two-dimensional recursively filtered signals," in *Proceedings of the International Conference on Acoustics, Speech, and Signal Processing*, 1984, pp. 20.11.1-20.11.4.
3. S. J. Ko and Y. H. Lee, "Center weighted median filters and their applications to image enhancement," *IEEE Transactions on Circuits and Systems*, Vol. 38, 1991, pp. 984-933.
4. T. Chan, K. K. Ma, and L. H. Chen, "Tri-state median filter for image de-noising," *IEEE Transactions on Image Processing*, Vol. 8, 1999, pp. 1834-1838.
5. T. Chen and H. R. Wu, "Impulse noise removal by multi-state median filtering," in *Proceedings of the International Conference on Acoustics, Speech, and Signal Processing*, 2000, pp. 2183-2186.
6. G. R. Arce and J. L. Paredes, "Recursive weighted median filters admitting negative weights and their optimization," *IEEE Transactions on Signal Processing*, Vol. 48, 2000, pp. 768-779.
7. H. M. Lin and A. N. Willson, "Median filters with adaptive length," *IEEE Transactions on Circuits and Systems*, Vol. 35, 1988, pp. 675-690.
8. M. P. McLoughlin and G. R. Arce, "Deterministic properties of the recursive separable median filter," *IEEE Transactions on Acoustics, Speech, Signal Processing*, Vol. ASSP-35, 1987, pp. 98-106.
9. G. Qiu, "An improved recursive median filtering scheme for image processing," *IEEE Transactions on Image Processing*, Vol. 5, 1996, pp. 646-648.
10. D. A. F. Florencio and R. W. Schafer, "Decision-based median filter using local signal statistics," in *Proceedings of the SPIE Symposium on Visual Communications Image Processing*, Vol. 2308, 1994, pp. 268-275.
11. C. T. Chen and L. G. Chen, "A self-adjusting weighted median filter for removing impulse noise in image," in *Proceedings of the IEEE International Conference on Image Processing*, 1998, pp. 419-422.
12. G. Pok and J. C. Liu, "Decision-based median filter improved by predictions," in *Proceedings of the IEEE International Conference on Image Processing*, 1999, pp. 410-413.
13. X. Li and M. Orchard, "True edge-preserving filtering for impulse noise removal," in *Proceedings of 34th Asilomar Conference on Signals, Systems and Computers*, Pacific Grove C, Oct. 2000.
14. C. H. Chou and Y. C. Li, "A perceptually tuned subband image coder based on the measure of just-noticeable-distortion profile," *IEEE Transactions on Fuzzy Systems*, Vol. 3, 1995, pp. 467-476.

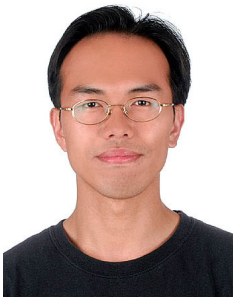

Shih-Mao Lu (盧世茂) received the B.E. degree from National Tsing Hua University in Power Mechanical Engineering and the M.E. degree from National Chiao Tung University in Electrical Eontrol Engineering, Hsinchu, Taiwan, R.O.C., in 1998 and 2000, respectively. He is currently pursuing the Ph.D. degree from National Chiao Tung University in Electrical Control Engineering. His research interests include image processing, noise and compression coding artifacts suppression, visual quality assessment, human vision system, and applications of neural networks and fuzzy theory.

Sheng-Fu Liang (梁勝富) was born in Tainan, Taiwan, in 1971. He received the B.S. and M.S. degrees in Electrical and Control Engineering from the National Chiao Tung University (NCTU), Taiwan, in 1994 and 1996, respectively. He received the Ph.D. degree in Electrical and Control Engineering from NCTU in 2000. From 2001 to 2005, he was a Research Assistant Professor in Electrical and Control Engineering, NCTU. In 2005, he joined the Department of Biological Science and Technology, NCTU, where he serves as an Assistant Professor. Dr. Liang has also served as the chief executive of Brain Research Center, NCTU Branch, University System of Taiwan since September 2003. His current research interests are biomedical engineering, biomedical signal/image processing, machine learning, fuzzy neural networks (FNN), the development of brain-computer interface (BCI), and multimedia signal processing.

Chin-Teng Lin (林進燈) received B.S. degree from National Chiao Tung University (NCTU), Taiwan in 1986 and Ph.D. degrees in Electrical Engineering from Purdue University, U.S.A., in 1992. He is currently the Chair Professor and Associate Dean of the College of Electrical Engineering and Computer Science, and Director of Brain Research Center at NCTU. Dr. Lin is the author of Neural Fuzzy Systems (Prentice Hall). He has published about 90 journal papers including over 65 IEEE journal papers. Dr. Lin is an IEEE Fellow for his contributions to biologically inspired information systems. He serves on Board of Governors at IEEE CAS and SMC Societies now. He has been the President of Asia Pacific Neural Network Assembly since 2004. Dr. Lin has received the Outstanding Research Award granted by National Science Council, Taiwan, since 1997 to present, the Outstanding Engineering Professor Award granted by the Chinese Institute of Engineering (CIE) in 2000, and the 2002 Taiwan Outstanding Information-Technology Expert Award. Dr. Lin was also elected to be one of the 38th Ten Outstanding Rising Stars in Taiwan (2000). Dr. Lin currently serves as Associate editors of IEEE Transactions on Circuits and Systems, Part I & Part II, IEEE Transactions on Systems, Man, Cybernetics, IEEE Transactions on Fuzzy Systems, etc.